Formation of $Cp(CO)(PR_3)FeCH(OCH_3)C_6H_5$ Complexes via PR_3 Substitution Reactions, Hydride Addition to $Cp(CO)(PR_3)Fe{=}C(OCH_3)C_6H_5^+$, and Methoxide Addition to $Cp(CO)(PR_3)Fe{=}CHC_6H_5^+$. Kinetic and Thermodynamic Diastereoselectivities. Relative Reactivities of Synclinal and Anticlinal Iron Carbene Isomers

M. Brookhart* and Robert C. Buck

Contribution from the Department of Chemistry, William Rand Kenan, Jr., Laboratories, The University of North Carolina at Chapel Hill, Chapel Hill, North Carolina 27514.

Received March 7, 1988

Abstract: Photosubstitution of $Cp(CO)_2FeCH(OCH_3)C_6H_5$ (**3**) by PPh_3 at 25 °C gives $Cp(CO)(PPh_3)FeCH(OCH_3)C_6H_5$ (**4**) with high diastereoselectivity ((*SR*)-**4**:(*RS*)-**4** to (*SS*)-**4**:(*RR*)-**4** ca. 75:1). The substitution proceeds via the η^3-benzyl complex $Cp(CO)Fe(\eta^3\text{-}CH(OCH_3)C_6H_5)$ (**9**). When **9** is trapped at −50 °C, kinetically low diastereoselectivity is observed ((*SR*)-**4**:(*RS*)-**4** to (*SS*)-**4**:(*RR*)-**4** ca. 2:1). Upon warming, (*SS*)-**4**:(*RR*)-**4** isomerizes to (*SR*)-**4**:(*RS*)-**4** via PPh_3 dissociation–reassociation. Rates of isomerization and PPh_3 dissociation were measured, and a quantitative free energy diagram for diastereomer interconversion was constructed. Photosubstitution of optically active (*R*)-**3** yields racemic (*SR*)-**4**:(*RS*)-**4**. A mechanism for racemization of Cα involving α-elimination is proposed. Photosubstitution of **3** by PEt_3 at 25 °C yields two configurationally stable diastereomers of $Cp(CO)(PEt_3)FeCH(OCH_3)C_6H_5$ ((*SR*)-**7**:(*RS*)-**7** to (*SS*)-**7**:(*RR*)-**7** ca. 3:2). Photosubstitution of optically active (*R*)-**3** by PEt_3 yields diastereomers of **7** with high optical rotations and presumably high optical purity ((*SR*)-**7** and (*RR*)-**7**). Methoxide addition to $Cp(CO)(PR_3)Fe{=}CHC_6H_5^+$ ($PR_3 = PPh_3$ (**11**) and PEt_3 (**12**)) yields both diastereomers in significant amounts. In each case diastereomer ratios are dependent on methoxide concentration. The minor synclinal benzylidene isomers, *syn*-**11** and -**12**, are more reactive than the major anticlinal isomers, *anti*-**11** and -**12**. Curtin–Hammett kinetics are used to analyze these results. Hydride additions to $Cp(CO)(PR_3)Fe{=}C(OCH_3)C_6H_5^+$ (PPh_3 (**17**) and PEt_3 (**18**)) give mixtures of diastereomers whose ratios are independent of BH_4^- concentrations.

$Cp(NO)(PPh_3)Re$ and $Cp(CO)(PPh_3)Fe$ ($Cp = \eta^5\text{-}C_5H_5$) have recently been used as chiral auxiliaries to carry out numerous diastereoselective and enantioselective transformations.[1-4] Our interest in such complexes has centered primarily on the reactions of enantiomerically pure chiral-at-iron carbene complexes of the type $Cp(CO)(PR_3)Fe{=}CHR^+$. These complexes transfer the carbene moiety to alkenes to give cyclopropanes often with high enantioselectivity:[5]

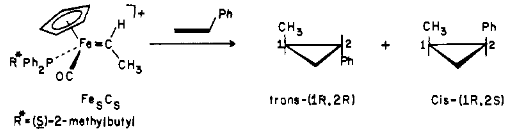

Precursors to optically pure carbene complexes are optically pure α-ether complexes of the general structure $Cp(CO)(PR_3)$-$FeCH(OMe)R$, which can be converted to carbene complexes via ionization of methoxide with electrophiles, normally $(CH_3)_3SiOTf$. A current limitation to more extensive use of chiral iron carbene complexes is the lack of general routes to optically pure α-ether complexes.

In studies directed toward developing syntheses of optically pure chiral-at-iron benzylidene complexes $Cp(CO)(PR_3)Fe^*{=}CHC_6H_5^+$, we have examined several routes to diastereomers **1** and **2**, which serve as precursors to benzylidene complexes. The

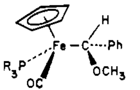

1

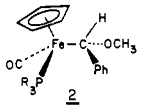

2

routes investigated include photochemical carbonyl substitution in $Cp(CO)_2FeCH(OCH_3)C_6H_5$ (**3**) by phosphines, methoxide addition to the benzylidene complexes $Cp(CO)(PR_3)Fe{=}CHC_6H_5^+$, and hydride addition to the heteroatom carbene complexes $Cp(CO)(PR_3)Fe{=}C(OCH_3)C_6H_5^+$ (R = Ph, Et).

We report here the results of these investigations, several features of which bear directly on general, fundamental questions of diastereoselectivity in these systems including (a) the relative reactivities of the synclinal and anticlinal carbene isomers, (b) the ability of a chiral carbon center, adjacent to a prochiral iron center, to induce diastereoselective carbonyl substitution with

---

(1) Leading references of work by Gladysz: (a) Georgiou, S.; Gladysz, J. A. *Tetrahedron* **1986**, *42*, 1109. (b) Fernandez, J. M.; Gladysz, J. A. *Inorg. Chem.* **1986**, *25*, 2672. (c) Smith, D. E.; Gladysz, J. A. *Organometallics* **1985**, *4*, 1480. (d) Merrifield, J. H.; Fernandez, J. M.; Buhro, W. E.; Gladysz, J. A. *Inorg. Chem.* **1984**, *23*, 4022. (e) Grocco, G. L.; Gladysz, J. A. *J. Chem. Soc., Chem. Commun.* **1986**, 1154. (f) Kiel, W. A.; Lin, G.-Y.; Constable, A. G.; McCormick, F. B.; Strouse, C. E.; Eisenstein, O.; Gladysz, J. A. *J. Am. Chem. Soc.* **1982**, *104*, 4865.

(2) (a) Davies, S. G.; Dordor-Hedgecock, I. M.; Sutton, K. H.; Whittaker, M. *J. Organomet. Chem.* **1987**, *320*, C19. (b) Ayscough, A. P.; Davies, S. G. *J. Chem. Soc., Chem. Commun.* **1986**, 1648. (c) Davies, S. G.; Maberly, T. M. *J. Organomet. Chem.* **1985**, *296*, C37. (d) Baird, G. J.; Davies, S. G.; Maberly, T. R. *Organometallics* **1984**, *3*, 1764.

(3) (a) Seeman, J. I.; Davies, S. G. *J. Am. Chem. Soc.* **1985**, *107*, 6533. (b) Davies, S. G.; Seeman, J. I. *Tetrahedron Lett.* **1984**, 1845. (c) Seeman, J. I.; Davies, S. G. *J. Chem. Soc., Chem. Commun.* **1984**, 1019. (d) A recent analysis of the benzyl system $Cp(CO)(PPh_3)FeCH_2Ph$ suggests two conformations are present. The major conformer is **13** (R′ = Ph), while the minor conformer is proposed as one in which phenyl and Cp groups are eclipsed. These results are consistent with conclusions drawn here concerning assignments of diastereomer configurations: Davies, S. G.; Dordor-Hedgecock, I. M.; Sutton, K. H.; Whittaker, M. *J. Am. Chem. Soc.* **1987**, *109*, 5711.

(4) (a) Liebeskind, L. S.; Welker, M. E. *Tetrahedron Lett.* **1984**, *25*, 4311. (b) Liebeskind, L. S.; Welker, M. E.; Goedken, V. *J. Am. Chem. Soc.* **1984**, *106*, 441. (c) Liebeskind, L. S.; Welker, M. E. *Organometallics* **1983**, *2*, 195. (d) Brinkman, K.; Helquist, P. *Tetrahedron Lett.* **1985**, *26*, 2845.

(5) (a) Brookhart, M.; Timmers, D.; Tucker, J. R.; Williams, G. D.; Husk, G. R.; Brunner, H.; Hammer, B. *J. Am. Chem. Soc.* **1983**, *105*, 6721. (b) Brookhart, M.; Tucker, J. R.; Husk, G. R. *Ibid.* **1983**, *105*, 258. (c) Brookhart, M.; Studebaker, W. *Chem. Rev.* **1987**, *87*, 411. (d) Buck, R. C.; Brookhart, M. *Abstracts of Papers*, 191st National Meeting of the American Chemical Society, New York, April 13–18, 1986; American Chemical Society: Washington, DC, 1986; INORG 422. (e) For early work regarding enantioselective reactions of $Cp(CO)(PPh_3)Fe{=}CH_2^+$, see: Davidson, A.; Krussell, W. C.; Michaelson, R. C. *J. Organomet. Chem.* **1974**, *72*, C7. Flood, T. C.; DiSanti, F. J.; Miles, D. L. *Inorg. Chem.* **1972**, *15*, 1910.

0002-7863/89/1511-0559$01.50/0 © 1989 American Chemical Society

phosphines, (c) the role of η^3-benzyl derivatives in carbonyl substitution reactions and loss of configuration at C_α, and (d) the relative thermodynamic stabilities and configurational stability at iron of complexes $Cp(CO)(PPh_3)FeCH(OCH_3)C_6H_5$ (**4**) and $Cp(CO)(PEt_3)FeCH(OCH_3)(C_6H_5)$ (**7**). Part of this work has been communicated.[6] Spectroscopic studies of η^3-benzyl intermediates appear in the following paper.[7]

Results and Discussion

A. Photochemical Substitution of CO by PR$_3$. Photolysis of racemic $Cp(CO)_2FeCH(OCH_3)C_6H_5$ (**3**) at 0 °C in C_6H_6 in the presence of excess PPh_3 results (after workup at 25 °C) in carbonyl substitution to form $Cp(CO)(PPh_3)FeCH(OCH_3)C_6H_5$ (**4**) as a single diastereomeric product (*SR*)-**4**:(*RS*)-**4** (eq 1). (Config-

$$\underset{\underline{3}}{Cp(CO)_2FeCH(OCH_3)C_6H_5} \xrightarrow[\text{Hexanes, 0°C}]{PPh_3,\ h\nu} \underset{\underline{4}}{Cp(CO)(PPh_3)FeCH(OCH_3)C_6H_5} \qquad (1)$$

urational assignments will be documented below.) The other possible diastereomer (*SS*)-**4**:(*RR*)-**4** was not apparent in the ^{1}H or ^{13}C NMR spectrum of the reaction product (i.e. <2%), indicating highly diastereoselective carbonyl substitution (>98%). In eq 2 and 3 the four possible diastereomeric products arising from

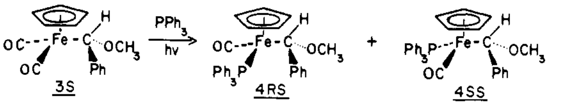

(2)

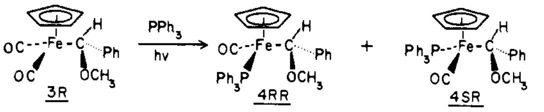

(3)

carbonyl substitution of **3** with PPh_3 are considered. As is apparent, if a single enantiomer of **3** (i.e. (*R*)-**3** or (*S*)-**3**) could be prepared, then the product arising from PPh_3 substitution would be a single enantiomer of the sole product diastereomer (i.e. (*R*)-**3** ⇒ (*SR*)-**4** *only*). Such a species would represent a precursor to optically pure chiral-at-iron benzylidene complexes.

The strategy employed for synthesizing enantiomerically pure complexes of **3** is shown in eq 4 and utilizes a chiral α-methoxy

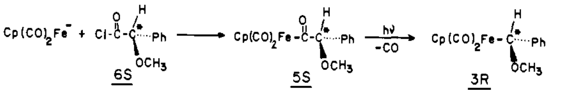

(4)

acid chloride **6** derived from mandelic acid $C_6H_5C^*H(OH)-COOH$. Treatment of $Cp(CO)_2Fe^-M^+$ with optically pure (*S*)-α-methoxymandeloyl chloride ((*S*)-**6**) results in formation of the optically active acyl complex (*S*)-**5** in 85% isolated yield ($[\alpha]^{23}_D = -90°$). Photolysis of (*S*)-**5** at 0 °C in hexanes induces carbonyl loss followed by alkyl migration to give (*R*)-**3**. Whitesides[7] has investigated the carbonyl insertion and deinsertion reactions of numerous $Cp(CO)(L)FeR$ complexes ($R = -C^*HRR'$, $-COC^*HRR'$; $L = CO, PPh_3$) and found in all cases that the reactions proceeded with retention of stereochemistry at the migrating carbon. We assume that the above reaction also proceeds with retention of configuration at the migrating carbon. Photolysis of (*R*)-**3** in the presence of PPh_3 yields a single diastereomeric product. The reaction is performed more efficiently by photolyzing acyl (*S*)-**5** in the presence of PPh_3 with both photochemical steps done in one reaction vessel. Remarkably, the single diastereomeric product obtained was *racemic*, showing no optical rotation. This observation implies that racemization at Cα occurs during the course of the photochemical substitution of CO by PPh_3 (i.e. the racemic mixture (*SR*)-**4** *and* (*RS*)-**4** was obtained).

To determine if high diastereoselectivity and Cα racemization was a general phenomenon upon CO substitution by phosphines, a second phosphine, PEt_3, was examined. Photolysis of (*S*)-**5** at 0 °C in hexanes in the presence of excess PEt_3 yields a 3:2 mixture of the diastereomeric complexes (*SR*)-**7** and (*RR*)-**7**, respectively (eq 5). These complexes were separated by low-temperature

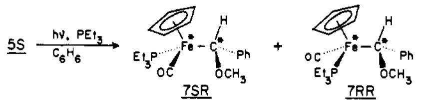

(5)

chromatography and had nearly equal but opposite optical rotations of $[\alpha]_{436} = -720°$ and $[\alpha]_{436} = +740°$, respectively, indicating that significant Cα racemization had *not* taken place. The enantiomeric purity of these complexes could not be determined; use of chiral shift reagents proved unsuccessful.[8,9] However, their optical rotations are of the magnitude reported for chiral-at-iron organometallic complexes of similar structure. Brunner[10] has tabulated optical rotations for a number of complexes $Cp(CO)(PPh_2R)Fe^*X$ and found that for optically pure complexes $[\alpha]_{436}$ = ca. +1000° (Fe_S) or $[\alpha]_{436}$ = ca. −1000° (Fe_R). These results suggest that the racemization process and high diastereoselection were characteristic of PPh_3 but *not* of photosubstitution of phosphines in general.

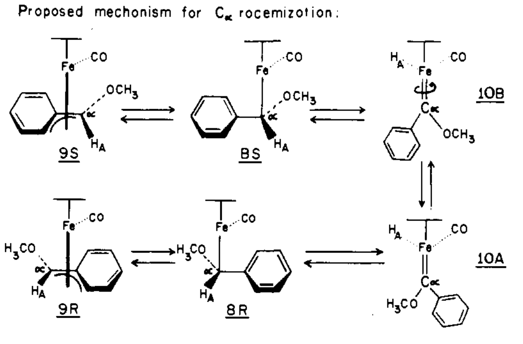

Figure 1.

Lability of PPh_3 in complex (*SR*)-**4**:(*RS*)-**4** was established by adding 6 equiv of PEt_3 to a C_6D_6 solution of (*SR*)-**4**:(*RS*)-**4** in the dark. At 25 °C in 5 h complete disappearance of (*SR*)-**4**:(*RS*)-**4** and loss of PPh_3 occurred accompanied by appearance of PEt_3 diastereomers (*SR*)-**7**:(*RS*)-**7** and (*SS*)-**7**:(*RR*)-**7** in the same 3:2 ratio as obtained from photolysis of (*S*)-**5**. This result suggests that the high diastereoselection observed for PPh_3 is a thermodynamic result since equilibration of diastereomers can occur rapidly via PPh_3 dissociation–reassociation at 25 °C. However, such a process in itself *cannot* account for racemization of the Cα carbon. PEt_3 complexes (*SR*)-**7**:(*RS*)-**7** and (*SS*)-**7**:(*RR*)-**7** are configurationally stable and do not interconvert at 25 °C nor undergo ligand exchange in the presence of other phosphine ligands.

To determine whether any intermediates could be observed, which would shed light upon the mechanism of Cα racemization, **3** was photolyzed in the absence of trapping ligands. Irradiation of a clear yellow solution of **3** at −80 °C in toluene-d_8 with a N_2 purge results in rapid CO loss and formation of a deep red solution. The product formed from collapse of the 16e unsaturated intermediate **8** is the iron η^3-benzyl complex **9** with the configuration shown[10] (eq 6). Similar species $(\eta^5-C_5R_5)(CO)Fe(\eta^3-CH_2C_6H_5)$

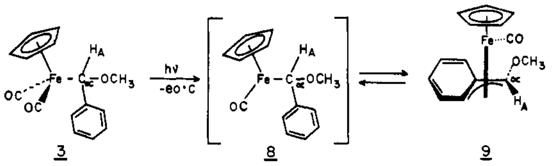

(6)

(R = H, Me) have been observed by Wrighton.[11] Complex **9**

---

(6) Brookhart, M.; Liu, Y.; Buck, R. C. *J. Am. Chem. Soc.* **1988**, *110*, 2337.

(7) See the following paper for the details of the synthesis configurational assignment, dynamic processes and rates of PR_3 (R = Et, Ph) trapping of $Cp(CO)Fe(\eta^3-CH(OCH_3)C_6H_5$ (**9**).

(8) Whitesides, G. M.; Boschetto, D. J. *J. Am. Chem. Soc.* **1969**, *91*, 4313.

(9) $Eu[hfc]_3$ was used in an attempt to determine enantiomeric purity but was unsuccessful.

(10) (a) Brunner, H.; Schmidt, E. J. *J. Organomet. Chem.*, **1972**, *36*, C18. (b) Brunner, H. *Adv. Organomet. Chem.* **1980**, *18*, 151. (c) Brunner, H.; Vogt, H. *J. Organomet. Chem.* **1980**, *191*, 181.

Table I. PR_3 Trapping of $Cp(CO)Fe[\eta^3\text{-}CH(OCH_3)C_6H_5]$

PR_3		^1H NMR			*SR*:*RS* to *SS*:*RR*
		δ-$CH\alpha$	δ-C_5H_5	δ-OCH_3	
PPh_3 (**4**)	major	5.17 (d), J_{PH} = 9.2 Hz	4.10 (s)	2.83 (s)	2:1
	minor	5.32 (d), J_{PH} = 6.9 Hz	3.83 (s)	2.30 (s)	
PEt_3 (**7**)	major	4.93 (d), J_{PH} = 8.9 Hz	4.07 (d), J_{PH} = 0.9 Hz	3.18 (s)	3:2
	minor	5.19 (d), J_{PH} = 6.9 Hz	3.78 (s)	3.07 (s)	

is a fluxional molecule. Variable-temperature ^1H NMR established site exchange of the ortho (H_o, $H_{o'}$) and meta (H_m, $H_{m'}$) protons on the phenyl ring via σ to π interconversions (ΔG^{*} = 15.4 kcal/mol).[10] However, the configuration at $C\alpha$ is not inverted by this process.[10]

A mechanism that may account for the racemization of $C\alpha$ is shown in Figure 1. Iron η^3-benzyl complex (*S*)-**9** undergoes $\sigma \rightarrow \pi$ conversion to form the 16e unsaturated η^1-benzyl complex (*S*)-**8**. α-Hydrogen migration occurs to yield carbene–hydride **10B**; rotation about the $C\alpha$–iron double bond forms **10A**, which undergoes migration of hydrogen from iron to $C\alpha$, yielding η^1-benzyl (*R*)-**8** in which inversion at $C\alpha$ has occurred. Complex (*R*)-**8** collapses to give (*R*)-**9** and the reversible process continues, ultimately yielding a racemic mixture of the two enantiomeric η^3-benzyl complexes (*S*)-**9** and (*R*)-**9**.

Numerous observations lend support to the proposed mechanism. η^3-Benzyl to η^1-benzyl interconversion is facile as confirmed by the dynamic process observed for complex **9**,[10] thus making the η^1-benzyl complex readily accessible. Migration of an α-hydrogen to a metal center to form a carbene–hydride has been observed by Dixneuf,[12] Winter,[13] Bercaw,[14] and Green.[15] The complexes reported by Green[15] and Bercaw[14] also undergo the reverse reaction, migration of the metal-bound hydrogen of the carbene–hydride complex back to the carbene carbon.

A very close analogy to the proposed **8** $\rightleftharpoons$ **10** equilibration is the rapid, reversible alkyl migration reaction demonstrated by Jones[16] and shown below:

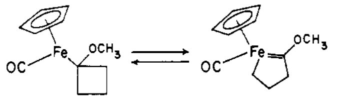

These results establish that rapid, reversible α-hydrogen migrations are very plausible processes in systems such as **8**. Resonance stabilization by the phenyl and methoxy substituents should diminish the $C\alpha$–iron double-bond character, making the barrier to rotation about the $C\alpha$–iron bond very low (i.e. <7 kcal/mol).[17]

To further probe the high diastereoselection observed for PPh_3 photosubstitution of **3** and lower diastereoselection for PEt_3, the products from trapping η^3-benzyl **9** with these ligands at low temperatures were determined. Complex **9** was generated at −80 °C in toluene-d_8 by photolysis of **3**. A total of 6 equiv of PPh_3 or PEt_3 was added at −80 °C and the sample monitored by ^1H NMR. The −80 °C spectrum of the reaction mixture showed no evidence of **4** or **7**, only the η^3-benzyl complex, indicating that **9** was inert to phosphine trapping at that temperature. The onset of ligand trapping occurred upon warming to ~−50 °C. The results of PPh_3 and PEt_3 trapping are summarized in Table I.[10] Trapping of **9** with PEt_3 forms a 3:2 mixture of diastereomers (*SR*)-**7**:(*RS*)-**7** and (*SS*)-**7**:(*RR*)-**7**, respectively, identical with the diastereoselectivity observed upon photolysis of (*S*)-**4** with PEt_3. Interestingly, trapping of **7** with PPh_3 yields a 2:1 mixture of diastereomers (*SR*)-**4**:(*RS*)-**4** and (*SS*)-**4**:(*RR*)-**4**, indicating that PPh_3 trapping is not *kinetically* highly diastereoselective. The (*SS*)-**4**:(*RR*)-**4** diastereomer, previously undetected, constituted 33% of the reaction product. In both cases, the major product is the *SR*:*RS* diastereomer having the higher field $CH\alpha$ signal with the larger $^3J_{PH}$, and lower field η^5-C_5H_5 and OCH_3 ^1H NMR signals.

When the 2:1 mixture of (*SR*)-**4**:(*RS*)-**4** and (*SS*)-**4**:(*RR*)-**4** was warmed to room temperature (293 K) and monitored, clean conversion of (*SS*)-**4**:(*RR*)-**4** into (*SR*)-**4**:(*RS*)-**4** was observed, ultimately yielding a ca. 75:1 equilibrium mixture of the two diastereomers as determined by ^1H NMR. *Diastereomer* interconversion via loss of configuration at iron occurs by PPh_3 dissociation–reassociation. However, inversion of configuration at $C\alpha$ (presumably by the mechanism detailed in Figure 1) must occur along with PPh_3 dissociation–reassociation in order to fully explain the racemic product (*SR*)-**4**:(*RS*)-**4** obtained from photolysis of (*S*)-**5** with PPh_3. Diastereomer interconversion by loss of configuration at $C\alpha$ does *not* occur by methoxide dissociation to form the benzylidene $Cp(CO)(PPh_3)Fe{=}CHC_6H_5^+$ **11** followed by methoxide readdition.[2d] No $-OCD_3$ incorporation is seen when $NaOCD_3/CD_3OD$ is added to the (*SR*)-**4**:(*RS*)-**4** and (*SS*)-**4**:(*RR*)-**4** diastereomer mixture generated from PPh_3 trap of **7** and diastereomer interconversion monitored to completion (i.e. 5 h at 293 K).

The rate of PPh_3 dissociation from (*SS*)-**4**:(*RR*)-**4** is 1.3 × 10^{-4} s^{-1} (T = 293 K, ΔG^{*}((*SS*)-**4**:(*RR*)-**4**) = 22.3 kcal/mol, $t_{1/2}$ = 87.5 min) and was measured as follows: The 2:1 (*SR*)-**4**:(*RS*)-**4** to (*SS*)-**4**:(*RR*)-**4** diastereomer mixture was generated at low temperature in toluene-d_8 by PPh_3 trapping of **9**. A total of 8 equiv of PEt_3 was added and the mixture warmed to 293 K. The solution was monitored by ^1H NMR and the rate determined by measuring the first-order disappearance of (*SS*)-**4**:(*RR*)-**4** and the appearance of the 3:2 mixture of (*SR*)-**7**:(*RS*)-**7** and (*SS*)-**7**:(*RR*)-**7**. The rate of PPh_3 dissociation from (*SR*)-**4**:(*RS*)-**4** is 3.1 × 10^{-6} s^{-1} (T = 293 K, ΔG^{*}((*SR*)-**4**:(*RS*)-**4**)) = 24.5 kcal/mol; $t_{1/2}$ = 61 h), 2 orders of magnitude slower than the rate of PPh_3 dissociation from (*SS*)-**4**:(*RR*)-**4**. The rate was measured as follows: The 75:1 (*SR*)-**4**:(*RS*)-**4**/(*SS*)-**4**:(*RR*)-**4** equilibrium mixture was dissolved in toluene-d_8, and 8 equiv of PEt_3 was added. The solution was monitored by ^1H NMR and the rate determined by measuring the first-order disappearance of (*SR*)-**4**:(*RS*)-**4** and appearance of the 3:2 mixture of (*SR*)-**7**:(*RS*)-**7** and (*SS*)-**7**:(*RR*)-**7**. (Since PEt_3 is known to trap the η^3-benzyl intermediate substantially faster than PPh_3,[10] it is safe to assume that in the presence of 8 equiv of PEt_3 essentially no back-reaction occurs and the rate-determining step is loss of PPh_3.)

The thermodynamic equilibrium ratio of (*SR*)-**7**:(*RS*)-**7** and (*SS*)-**7**:(*RR*)-**7** was found to be 3:2, the same ratio that was observed for kinetic trapping of **9** by PEt_3. This was established by adding a trace of acid to a 10:1 (*SR*)-**7**:(*RS*)-**7** to (*SS*)-**7**:(*RR*)-**7** diastereomer-enriched sample dissolved in CD_3OD.[18]

---

(11) Wrighton, M. S.; Blaha, J. P. *J. Am. Chem. Soc.* **1985**, *107*, 2345.

(12) Dixneuf, P. H.; Le Bozec, H.; Fillaut, J.-L. *J. Chem. Soc., Chem. Commun.* **1986**, 1182.

(13) (a) Winter, M. J.; Osborn, V. A.; Parker, C. A. *J. Chem. Soc., Chem. Commun.* **1986**, 1185. (b) Davey, C. E.; Osborn, V. A.; Parker, C. A.; Winter, M. J.; Woodward, S. *Abstracts of Papers*, 193rd National Meeting of the American Chemical Society, Denver, CO, April 5–10, 1987; American Chemical Society: Washington, DC, 1986; INORG 28.

(14) Bercaw, J. E.; Threlkel, R. S. *J. Am. Chem. Soc.* **1981**, *103*, 2650.

(15) (a) Green, M. L. H.; Cooper, N. J. *J. Chem. Soc., Dalton Trans.* **1979**, 1121. (b) Green, M. L. H.; Cooper, N. J. *Ibid.* **1982**, 1789.

(16) (a) Stenstrom, Y.; Klauck, G.; Koziol, A.; Palenik, G.; Jones, W. M. *Organometallics* **1986**, *5*, 2155. (b) Stenstrom, Y.; Jones, W. M. *Ibid.* **1986**, *5*, 178. (c) Lisko, J. R.; Jones, W. M. *Ibid.* **1985**, *4*, 944. (d) Svenstrom, Y.; Kozoil, A. E.; Palenik, G. J.; Jones, W. M. *Organometallics* **1987**, *6*, 2079.

(17) Brookhart, M.; Studabaker, W. B.; Husk, G. R. *Organometallics* **1985**, *4*, 943.

(18) Equilibration of (*SR*)-**5**:(*RS*)-**5** and (*SS*)-**5**:(*RR*)-**5** was also observed to occur when a diastereomer-enriched sample was dissolved in CD_3OD, but a small amount of insoluble decomposition product was present. This demonstrated the sensitivity of these complexes to traces of acidic impurities.

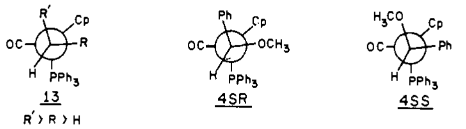

Figure 2.

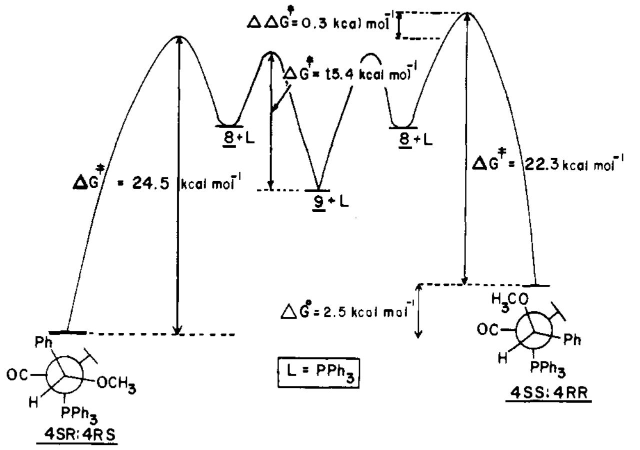

Figure 3.

Complete $-OCD_3$ incorporation occurred within 1 h together with equilibration to a 3:2 ratio of (*SR*)-**7**:(*RS*)-**7** to (*SS*)-**7**:(*RR*)-**7**. Pure samples of **7** dissolved in rigorously pure CD_3OD showed no $-OCD_3$ incorporation when kept in the dark and monitored for 24 h. Addition of 1 equiv of H^+ to a CD_3OD solution of **7** forms a deep red solution of $Cp(CO)(PEt_3)Fe{=}CHC_6H_5^+$ (**12**).

Configurational Assignment of Diastereomers $Cp(CO)(PR_3)FeCH(OCH_3)C_6H_5$. Davies and Seeman[3] have developed a model to predict the most stable conformation of $Cp(CO)(PPh_3)FeCHRR'$ [R' > R > H] complexes based upon molecular orbital calculations and X-ray crystallographic data. Their model predicts, as shown in **13** (Figure 2), that the smallest substituent (H) always occupies the most sterically hindered site between CO and PPh_3. The least sterically hindered site lies between cyclopentadienyl and CO. (Experimental evidence for this contention has been reported by Gladysz[1e] and Davies.[2b]) Thus, the most stable diastereomer is illustrated by **13** where the bulkiest group R' occupies this site. When Seeman and Davies' model is applied, diastereomers (*SR*)-**4**:(*RS*)-**4** and (*SS*)-**4**:(*RR*)-**4** will adopt the conformations shown in Figure 2. A phenyl group is sterically larger than $-OCH_3$,[19] therefore (*SR*)-**4**:(*RS*)-**4** is expected to be the more thermodynamically stable diastereomer.[3d]

The ground-state energy difference (ΔG°) between diastereomers (*SR*)-**4**:(*RS*)-**4** and (*SS*)-**4**:(*RR*)-**4** is 2.5 kcal/mol (K_{eq} = ca. 75:1). The energetics of the interconversion of the (*SR*)-**4**:(*RS*)-**4** and (*SS*)-**4**:(*RR*)-**4** diastereomers are summarized in the free energy diagram in Figure 3. The value $\Delta\Delta G^{\ddagger} = 0.3$ kcal/mol is calculated from the ground-state energy difference between (*SR*)-**4**:(*RS*)-**4** and (*SS*)-**4**:(*RR*)-**4** ($\Delta G^\circ = 2.5$ kcal/mol, K_{eq} = 75:1) and the rates of PPh_3 dissociation from (*SR*)-**4**:(*RS*)-**4** and (*SS*)-**4**:(*RR*)-**4** [i.e. $\Delta\Delta G^{\ddagger} = (\Delta G^{\ddagger}(SS)\text{-}4{:}(RR)\text{-}4) + \Delta G^\circ) - \Delta G^{\ddagger}((SR)\text{-}4{:}(RS)\text{-}4)$] and is consistent with $\Delta\Delta G^{\ddagger}$ calculated from the 2:1 kinetic ratio of (*SR*)-**4**:(*RS*)-**4** and (*SS*)-**4**:(*RR*)-**4** formed by trapping η^3-benzyl **9** with PPh_3.[10] Clearly, the differences in rates of PPh_3 dissociation from (*SR*)-**4**:(*RS*)-**4** and (*SS*)-**4**:(*RR*)-**4** are almost entirely due to their ground-state energy difference because $\Delta\Delta G^{\ddagger}$ is small.

The configurational assignment of the PEt_3 diastereomers (*SR*)-**7**:(*RS*)-**7** and (*SS*)-**7**:(*RR*)-**7** is made on the basis of the direct correlation of their ^1H NMR spectral data to that observed for (*SR*)-**4**:(*RS*)-**4** and (*SS*)-**4**:(*RR*)-**4**, respectively (see Table I). In both cases the more stable *SR*:*RS* diastereomer has the higher field $CH\alpha$ signal with the larger $^3J_{PH}$, and lower field η^5-C_5H_5 and OCH_3 ^1H NMR signals. (These assignments are not totally certain based upon this ^1H NMR correlation but are confirmed by the results of the methoxide quenching reactions discussed later.) The ground-state energy difference (ΔG°) between diastereomers (*SR*)-**7**:(*RS*)-**7** and (*SS*)-**7**:(*RR*)-**7** (0.24 kcal/mol) is too small to use as a basis for the configurational assignments of (*SR*)-**7**:(*RS*)-**7** and (*SS*)-**7**:(*RR*)-**7** and is probably due to a significant decrease in steric crowding (PEt_3 cone angle = 132°; PPh_3 cone angle = 145°). The smaller size and better donor properties of PEt_3 relative to PPh_3 results in configurationally stable PEt_3 complexes (*SR*)-**7**:(*RS*)-**7** and (*SS*)-**7**:(*RR*)-**7** that do not undergo rapid phosphine dissociation–reassociation.

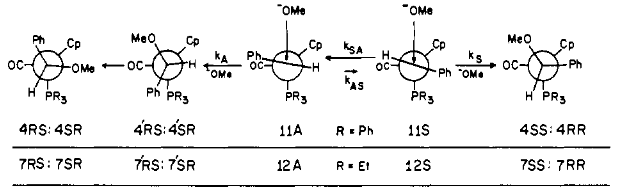

Figure 4.

B. Methoxide Addition to Benzylidene Complexes. Another potential route to achieve diastereoselective synthesis of $Cp(CO)(PR_3)FeCH(OCH_3)C_6H_5$ (**4**, R = Ph; **7**, R = Et) complexes is via methoxide addition to the cationic iron benzylidene complexes $Cp(CO)(PPh_3)Fe{=}CHC_6H_5^+$ (**11**) and $Cp(CO)(PEt_3)Fe{=}CHC_6H_5^+$ (**12**) (Figure 4). Extended Hückel calculations[20] and extensive spectroscopic and structural studies by Glasysz[1] on the isoelectronic $Cp(NO)(PPh_3)Re{=}CHPh^+$ complex (**14**) and analogues (i.e. $Cp(NO)(PPh_3)Re{=}CHR^+$) show that the carbene fragment is inclined such that it is aligned with the rhenium–nitrosyl bond. The two possible rotamers are termed *anti*-**11** and -**12** and *syn*-**11** and -**12** (Figure 4). Gladysz[1] has also shown that the anticlinal benzylidene isomer *anti*-**14** is the thermodynamically more stable (anticlinal:synclinal > 99:1) and that nucleophilic attack occurs exclusively over the smaller NO ligand of *anti*-**14** on the face opposite PPh_3. In addition, extended Hückel calculations by Seeman and Davies[3] show a general correlation in conformational structure and reactivity patterns for $Cp(CO)(PPh_3)Fe{=}CRR'^+$ and $Cp(NO)(PPh_3)Re{=}CRR'^+$ complexes and $Cp(CO)(PPh_3)Fe$-alkyl and $Cp(CO)(PPh_3)Re$-alkyl complexes. On the basis of these results, addition of methoxide to the electrophilic benzylidene complexes **11** and **12** should proceed by attack of methoxide over CO (anti to PR_3). If the product is formed from the thermodynamically more stable anticlinal isomers (*anti*-**11** and -**12**), the *SR*:*RS* diastereomer should be the major product. However, unlike the rhenium benzylidene complex **14**, which has a substantial barrier to isomer interconversion, in the iron benzylidenes **11** and **12** the synclinal and anticlinal isomers are no doubt in very rapid equilibrium ($\Delta G^{\ddagger} < 7$ kcal/mol). Therefore, invoking the Curtin–Hammett principle, there is no certainty that products from methoxide addition will arise solely from the thermodynamically favored anticlinal benzylidene isomer.

Complex **11** was generated at −78 °C in CD_2Cl_2 by adding 1 equiv of CF_3COOH to **4**. The deep red solution of **11** was added dropwise to a CD_3OD/CD_3ONa solution (>5 equiv of $NaOCD_3$ relative to CF_3COOH) in a 5-mm NMR tube cooled to 0 °C, which was being purged with nitrogen to facilitate rapid mixing. Immediate discharge of the deep red color of **11** to clear orange occurs upon addition. After addition, all samples were immediately cooled to −78 °C and sealed under vacuum. ^1H NMR spectra were recorded at −42 °C to determine the product diastereomer ratios. NMR tube manipulations at low temperatures were necessary to prevent diastereomer interconversion by processes described earlier. Methoxide addition to **12** was done in a similar manner but on a preparative scale with magnetic stirring of the methoxide solution. Low-temperature manipulations were not

---

(19) Eliel, E. L.; Allinger, N. L.; Angyal, S. J.; Morrison, G. A. *Conformational Analysis*; Interscience: New York, 1965; p 44.

(20) Extended Hückel calculations on the $Cp(CO)(PH_3)Fe$ fragment suggest an inclined conformation for the carbene ligand with it aligned with the metal–carbonyl bond. Schilling, B. E. R.; Hoffman, R.; Faller, J. W. *J. Am. Chem. Soc.* **1979**, *101*, 592.

Table II. Methoxide Addition to $Cp(CO)(PR_3)Fe{=}CHPh^+$

entry	R	[$NaOCH_3$], M	*SR*:*RS* to *SS*:*RR*
1	Ph	4.0	4.2:1.0
2	Ph	2.0	1.9:1.0
3	Ph	1.0	1.1:1.0
4	Ph	0.2	1.0:1.6
5	Et	2.0	5.0:1.0
6	Et	1.0	4.0:1.0
7	Et	0.5	3.0:1.0

[a] All quenches were done at 0 °C.

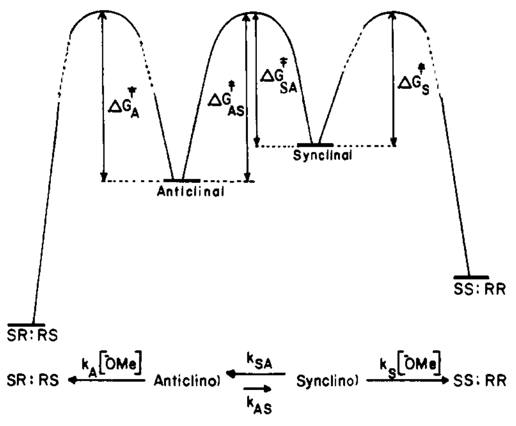

Figure 5.

necessary because diastereomers (*SR*)-**7**:(*RS*)-**7** and (*SS*)-**7**:(*RR*)-**7** are configurationally stable. The diastereomer ratios of products of **7** were determined by ^1H NMR at ambient temperature.

The results of methoxide addition to **11** and **12** at various concentrations are summarized in Table II and show that the observed diastereoselectivity is dependent upon methoxide concentration. The model that best accounts for these results is shown in Figure 5 and employs the Curtin–Hammett principle. The intrinsic reactivity of the synclinal isomer is assumed to be greater than the anticlinal isomer ($k_S > k_A$, $\Delta G^{\ddagger}_S < \Delta G^{\ddagger}_A$). The quenching rate ($k[^-OMe]$) is dependent upon methoxide concentration and thus so are $\Delta G^{\ddagger}_S$ and $\Delta G^{\ddagger}_A$. The rate of synclinal $\rightleftharpoons$ anticlinal interconversion is first order and independent of methoxide concentration. In the case of **11**, at low methoxide concentration (0.2 M), the rate of interconversion is sufficiently fast relative to quenching (i.e. $k_{A\to S} > k_A$, k_S and $\Delta G^{\ddagger}_{A\to S} < \Delta G^{\ddagger}_A$, $\Delta G^{\ddagger}_S$) that the major product arises from the more reactive but less populated synclinal isomer. As methoxide concentration increases, the rate of quenching increases ($\Delta G^{\ddagger}_S$ and $\Delta G^{\ddagger}_A$ decrease), and the [anticlinal]/[synclinal] ratio becomes increasingly more important in determining the product ratio. Thus, progressively more product arises from the major anticlinal isomer.[21]

A similar argument applies to the reaction of PEt_3 complex **12** in which we have established that [*anti*-**12**]/[*syn*-**12**] ≥ 30 (see below). Again, the diastereomer ratio is concentration dependent, and as methoxide concentration is decreased increasingly more product arises from the synclinal isomer. However, at the lowest concentration used (0.5 M), the (*SR*)-**7**:(*RS*)-**7** diastereomer still predominates (3:1) and the higher reactivity of the synclinal isomer does not counterbalance the high anticlinal/synclinal ratio (≥30:1). The diastereomers whose yields increase with increasing [^-OMe] must be those from trapping anticlinal isomers, i.e., *anti*-**11** and *anti*-**12**. Thus, quenching results support our earlier configurational assignments of diastereomers **4** and **7**.

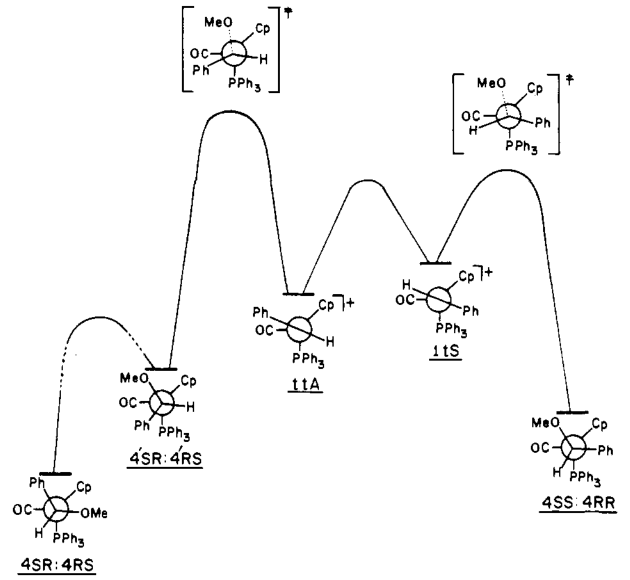

Figure 6.

The conformational analysis of Davies and Seeman[3] suggests a clear explanation for the higher reactivity of the synclinal isomers toward nucleophiles. This explanation arises from an analysis of the transition states and the initially generated product conformations from methoxide addition to the anticlinal and synclinal isomers *anti*-**11** and *syn*-**11** (Figure 6). Consider the transition state for attack on the anticlinal isomer *anti*-**11**. As methoxide approaches and Cα rehybridizes from sp^2 to sp^3, the bulkiest substituent at Cα, the phenyl group, must bend into the most sterically crowded site between CO and PPh_3. This transition state is thus highly sterically crowded. On the other hand, in the transition state for attack on the synclinal isomer *syn*-**11**, the smallest substituent at Cα, hydrogen, bends into its most favorable site between CO and PPh_3 making it less crowded and energetically more favorable than the transition state for *anti*-**11**.

Determination of Anticlinal/Synclinal Equilibrium Ratios for Cationic Iron Benzylidenes 11 and 12. To confirm the assumption that the equilibrium ratio of the synclinal and anticlinal benzylidene isomers of **11** and **12** were in fact highly biased toward the anticlinal isomer in analogy to the rhenium benzylidene **14**,[1] an attempt to spectroscopically observe both isomers by low-temperature ^1H NMR and establish their equilibrium ratio was made. When the 17.48 and 17.04 ppm signals of Hα of **11** and **12**, respectively (prepared in CD_2Cl_2/SO_2ClF by addition of (TMS)OTf to **4** and **7**), were monitored by ^1H NMR, neither significant line broadening (i.e. <1 Hz) nor variation in chemical shift (i.e. <0.05 ppm) was observed upon cooling to 148 K (−125 °C). This result suggests a high [anticlinal]/[synclinal] equilibrium ratio (> ca. 15). If substantial amounts of each isomer were present and the barrier for interconversion were higher than ca. 7–8 kcal/mol, then both species should have been observed at low temperatures, especially since the chemical shifts for the Hα protons of the synclinal and anticlinal isomers differ substantially.[5] If the barrier is lower than 7–8 kcal/mol, then an average chemical shift value would be observed and significant temperature dependence of the chemical shift would be expected over the large range of temperatures studied. Although the results argue for a large anticlinal/synclinal equilibrium ratio, they give no information regarding barriers of interconversion. On the basis of numerous model systems,[5] this barrier is expected to be low (<7–8 kcal/mol) especially since charge can be delocalized into the aryl ring reducing the multiple-bond character of the Fe–Cα bond.

---

(21) Seeman, J. I. *Chem. Rev.* **1983**, *83*(2), 83–134. The addition of methoxide to benzylidenes **11** and **12** can be analyzed by Curtin–Hammett/Winstein–Holness kinetics. There are two limiting cases: (1) When $k_A[Nu^-]$, $k_S[Nu^-] \gg k_{A\to S}$, $k_{S\to A}$, a kinetic quench is obtained and the product ratio is equal to the synclinal/anticlinal isomer ratio. (2) When $k_{A\to S}$, $k_{S\to A} \gg k_A[Nu^-]$, $k_S[Nu^-]$, the product ratio is equal to the product of the equilibrium constant K and the ratio of the reaction rate constants $k_A[Nu^-]$ and $k_S[Nu^-]$. In both of these cases, the product ratio remains constant and is independent of nucleophile concentration. Clearly, this system is an intermediate case where, $k_{A\to S}$, $k_{S\to A} \approx k_A[Nu^-]$, $k_S[Nu^-]$. Since $k_{S\to A}$ and $k_{A\to S}$ remain constant, the product ratio will depend upon $k_A[Nu^-]$ and $k_S[Nu^-]$, which are proportional to nucleophile concentration. Therefore, the product ratio will vary with nucleophile concentration until reaching one of the limiting cases described above.[6]

Table III. Hydride/Deuteride Addition to $Cp(CO)(PEt_3)Fe{=}CRC_6H_5^+$ (R = H, D)

benzylidene		δ-C*H*D ^{1}H NMR	δ-CH*D* ^{2}H NMR	config assgnt	diast ratio major to minor
12	major	1.75 (d), J_{PH} = 8.8 Hz	2.30 (s)	(*SS*)-**15**:(*RR*)-**15**	30:1
	minor	2.30 (d), J_{PH} = 4.8 Hz	1.72 (s)	(*SR*)-**15**:(*RS*)-**15**	
[α-*D*]-**12**	major	2.32 (d), J_{PH} = 4.7 Hz	1.75 (s)	(*SR*)-**15**:(*RS*)-**15**	30:1
	minor	1.75 (d), J_{PH} = 8.6 Hz	2.32 (s)	(*SS*)-**15**:(*RR*)-**15**	

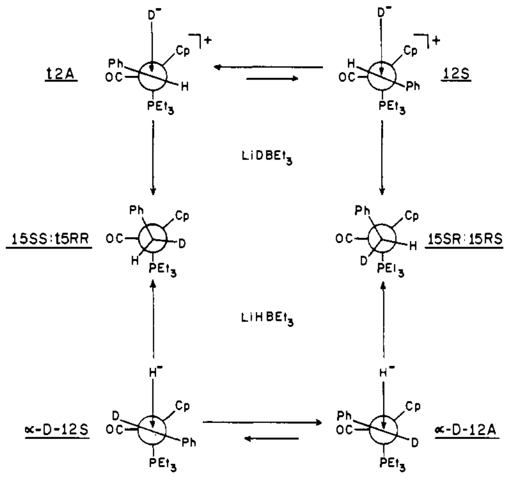

Figure 7.

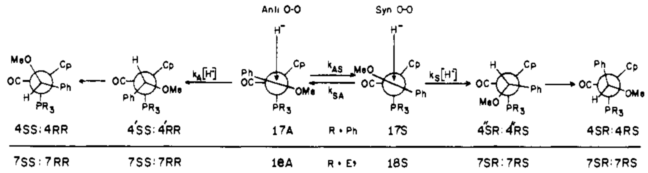

Figure 8.

Table IV. Hydride Addition to Heterocarbenes $Cp(CO)(PR_3)Fe{=}C(OMe)Ph^+$

entry	R	[NaBH$_4$], M	reaction *T*, °C	product diast *SS*:*RR* to *SR*:*RS* (±0.1)
1	Ph	1.0	0	1.0:1.0
2	Ph	0.4	0	1.2:1.0
3	Ph	0.4	−78	1.4:1.0
4	Ph	0.2	−78	1.3:1.0
5	Et	1.0	0	1.8:1.0
6	Et	0.2	0	1.7:1.0

Alternatively, a method to establish the equilibrium ratio by chemical means was pursued utilizing the conformational model **13** and arguments for assigning configuration detailed earlier (vide infra). A highly reactive nucleophile, which would add to the benzylidene isomers kinetically (i.e. faster than they interconvert), would give two diastereomeric products whose ratio would be identical with the equilibrium ratio of the synclinal and anticlinal isomers. The nucleophile chosen in this regard was hydride/deuteride. In parallel experiments, the benzylidenes **12** and [α-*D*)-**12** $Cp(CO)(PEt_3)Fe{=}CDC_6H_5^+$ were generated in CH_2Cl_2 and then added to rapidly stirred solutions of 1.0 M $LiDBEt_3$ or $LiHBEt_3$ in THF (−45 °C), respectively (Figure 7). The product diastereomers (*SS*)-**15**:(*RR*)-**15** and (*SR*)-**15**:(*RS*)-**15** were isolated in nearly quantitative yields and their ratios determined by ^{1}H and ^{2}H NMR. The results are shown in Table III. When the results and arguments discussed earlier are used, hydride/deuteride addition should occur over CO (anti to PEt_3) giving the diastereomers shown in Figure 7 (only one enantiomer of each is shown for clarity). The results reported here are exactly analogous to those reported by Gladysz for hydride/deuteride reduction of $Cp(NO)(PPh_3)Re{=}C(H \text{ or } D)C_6H_5^+$ complexes.[1f]

Recently, Davies[2a] has reported the X-ray crystal structure of $Cp(CO)(PPh_3)FeCH_2CH_3$ (**16**), which unequivocally showed that the bulkiest group at Cα (in this case $-CH_3$) prefers to occupy the R′ position in the most stable conformation as earlier Hückel calculations had predicted.[3] The methylene protons are diastereotopic and have very different $^3J_{PH}$ coupling constants (H_A, 12.1 Hz; H_B, 2.0 Hz). Using model **13** and applying the Karplus equation,[22] they concluded that a proton located between PPh_3 and CO (∠P–Fe–C–H = 30°) should have a larger $^3J_{PH}$ than a proton located between PPh_3 and cyclopentadienyl (∠P–Fe–C–H = 90°). On this basis, the ^{1}H NMR signals of the two Cα hydrogens were assigned.

From this information the location of the benzylic proton (–C*H*DPh) and the configurational assignment of the diastereomers (*SS*)-**15**:(*RR*)-**15** and (*SR*)-**15**:(*RS*)-**15** can be made on the basis of the observed $^3J_{PH}$ coupling constants for the products of the hydride/deuteride addition reactions.[3d] The major product observed in both experiments is from addition to the anticlinal benzylidene isomer. Since the amount of hydride/deuteride used was in large excess (>50-fold), we have assumed that addition is kinetic and accurately reflects a *minimum* value for the equilibrium ratio for *anti*-**12**/*syn*-**12** of >30:1.

Similar experiments attempted on the PPh_3 derivatives gave unsatisfactory results, possibly indicative of electron-transfer processes. For instance, addition of **11** to 1.0 M $LiDBEt_3$ at −45 °C gave $Cp(CO)(PPh_3)FeCH_2C_6H_5$ as the major reaction product. No conclusion concerning the equilibrium ratio of *anti*-**11** and *syn*-**11** could be drawn from the experiments. However, on the basis of comparisons of alkyl-substituted analogues, it is safe to assume that the equilibrium ratio of *anti*-**11** and *syn*-**11** strongly favors *anti*-**11**.

C. Hydride Addition to Heterocarbenes $Cp(CO)(PR_3)Fe{=}C(OCH_3)Ph^+$ (15, R = Ph; 16, R = Et). The third route investigated for diastereoselective synthesis of **4** and **7** was hydride addition to heterocarbene complexes $Cp(CO)(PPh_3)Fe{=}C\text{-}OCH_3)Ph^+$ (**17**) and $Cp(CO)(PEt_3)Fe{=}C(OCH_3)Ph^+$ (**18**). Davies[2d] has reported highly diastereoselective addition of hydride ($LiAlH_4$, $NaBH_4$ in THF) to $Cp(CO)(PPh_3)Fe{=}C(OCH_3)Et^+$ giving *SS*:*RR* $Cp(CO)(PPh_3)FeCH(OCH_3)Et$ (**19**) as the major product (15:1, *RR*:*SS* to *SR*:*RS*). To account for the diastereoselection, Davies proposed that (1) the methoxy group prefers the "anti(O–O)" conformation and (2) hydride adds exclusively to the anti(O–O) isomer on the face opposite to PPh_3. This reactivity pattern was proposed to be general (Rule 6, ref 3b). If this model applies to the present case, hydride addition to heterocarbene complexes *anti*-**17** and *anti*-**18** should give diastereomers (*SS*)-**4**:(*RR*)-**4** and (*SS*)-**7**:(*RR*)-**7** as the major products (Figure 8).

Complexes **17** and **18** were prepared by adding MeOTf to a CH_2Cl_2 solution of $Cp(CO)(PPh_3)FeCOC_6H_5$ (**20**) and $Cp(CO)(PEt_3)FeCOC_6H_5$ (**21**). Samples of **17** were dissolved in CD_2Cl_2 at room temperature, and the solution was then added dropwise to $CD_3OD/CD_3O^-Na^+/NaBH_4$ solutions in 5-mm NMR tubes of varied $NaBH_4$ concentration at either 0 or −78 °C.[23,24] Tubes were purged with N_2 to facilitate rapid mixing.

---

[22] Karplus, M. *J. Am. Chem. Soc.* **1963**, *85*, 2870.

[23] For the hydride quench reactions of **17** and **18** the molar ratio of $NaBH_4$ to $NaOCH_3$ or $NaOCD_3$ was 5:1.

After addition, samples were cooled to −78 °C, sealed under vacuum, and maintained at −78 °C until ^1H NMR spectra were recorded at −42 °C to determine the product **4** diastereomer ratios. Manipulations at low temperatures were necessary to prevent diastereomer interconversion by processes described earlier. Hydride addition to **18** was done similarly, but low-temperature manipulations were not required (vide infra). Product diastereomer ratios of **7** were determine by ^1H NMR at ambient temperature. Results of hydride addition to **17** and **18** are summarized in Table IV. The *SS*:*RR* diastereomer is the major product, but overall diastereoselection is low with little dependence on $NaBH_4$ concentrations or reaction temperatures.

The low diastereoselection may be explained in two possible ways: (1) Hydride addition is rapid relative to the rate of interconversion of the anti(O–O) and syn(O–O) isomers (i.e. $k_A[H^-]$, $k_S[H^-] > k_{AS}$, k_{SA}). The diastereomer ratios then reflect the anti(O–O) to syn(O–O) isomer ratios, indicating little difference in stability to the isomers. (2) The equilibrium favors the anti(O–O) isomer, but the rate of isomer interconversion is faster than the rate of hydride trapping (i.e. k_{AS}, $k_{SA} > k_A[H^-]$, $k_S[H^-]$). Diasteriomeric products are formed competitively through the minor, more reactive syn(O–O) isomer and the major, less reactive anti(O–O) isomer. As argued above, the syn(O–O) isomer is expected to be more reactive. In the transition state for hydride addition, the less sterically demanding methoxy substituent bends into the position between CO and PPh_3.

Both the barriers to isomer interconversion and reactivities of heterocarbene complexes **17** and **18** are expected to be lower than their benzylidene counterparts **11** and **12**. Resonance stabilization by the phenyl and methoxy groups significantly decreases the Fe–Cα multiple-bond character and electrophilicity of Cα. Thus, the barrier to rotation about the Fe–Cα bond of the heterocarbene will be less than its benzylidene analogue (i.e. <7 kcal/mol) with a corresponding decrease in reactivity due to diminished electrophilicity of Cα. These factors favor the second case as the more reasonable explanation for the observed diastereoselectivity.

Summary and Conclusions

Three synthetic approaches to $Cp(CO)(PR_3)FeCH(OCH_3)C_6H_5$ have been examined: (a) methoxide addition to benzylidene complexes, (b) hydride addition to phenyl methoxy carbene complexes, and (c) PR_3 substitution of the dicarbonyl complex $Cp(CO)_2FeCH(OCH_3)C_6H_5$. The results obtained provide fundamental information relative to the use of $Cp(CO)(PR_3)Fe$– moieties as chiral auxiliaries for carrying out stereoselective synthesis and the ability of a chiral Cα carbon to induce diastereoselective CO substitution.

Most significantly, addition of nucleophiles to carbene complexes of the type $Cp(CO)(PR_3)Fe{=}CHC_6H_5^+$ do not always proceed primarily through the dominant anticlinal carbene isomers. When nucleophilic addition is slower than carbene isomer interconversion, the Curtin–Hammett principle may apply and significant fractions of the addition products can arise from minor isomers. In the case of methoxide addition to $Cp(CO)(PR_3)Fe{=}CHC_6H_5^+$ (R = Ph, Et), the minor synclinal isomers are intrinsically more reactive than the anticlinal isomers and low diastereoselectivity is observed due to competitive reaction via both synclinal and anticlinal isomers. The higher intrinsic reactivities of the synclinal isomers are nicely accounted for by conformational analysis of $Cp(CO)(PR_3)FeCHRR'$ systems.[3] Diastereoselectivity is dependent upon methoxide concentration in these systems, which suggests methoxide addition (second order) and carbene isomer interconversion (first order) are competitive processes.

In reactions of the heterocarbene complexes $Cp(CO)(PR_3)Fe{=}C(OCH_3)C_6H_5^+$ with hydride donors, low diastereoselectivity is also noted contrary to the prediction of Seeman and Davies.[3b] Although the anti(O–O) isomer may predominate as suggested,[3b] it is clear that a substantial fraction of the reaction proceeds by hydride addition to the syn(O–O) isomer.

In light of these studies it is clear that the Curtin–Hammett principle must be considered in interpreting any of the diastereoselective reactions of $Cp(CO)(PR_3)Fe$ derivatives where isomer interconversion may compete with rates of reaction. A case in point are the carbene-transfer reactions carried out by reaction of alkenes with optically pure $Cp(CO)(PR_3)Fe{=}CHCH_3^+$ complexes.[5b] Knowing (a) that alkenes are weak nucleophiles and (b) that transfers are slower than carbene isomer interconversions and assuming that synclinal isomers are more reactive than anticlinal isomers suggest that high enantioselectivity results from alkene attack on the synclinal isomers. If this is the case, ring closure to form cyclopropanes occurs via a "backside closure" mechanism.[5b]

The high diastereoselectivity observed at 25 °C upon CO substitution by PPh_3 in $Cp(CO)_2FeCH(OCH_3)C_6H_5$ arises not from a kinetic selectivity but from a thermodynamic selectivity. PPh_3 dissociation from $Cp(CO)(PPh_3)FeCH(OCH_3)C_6H_5$ occurs readily in solution at 25 °C and allows diastereomer equilibration. Substitution and diastereomer interconversion occur via the η^3-benzyl intermediate $Cp(CO)Fe[\eta^3\text{-}CH(OCH_3)C_6H_5]$, detected by ^1H NMR spectroscopy.[10] Furthermore, when enantiomerically pure dicarbonyl (*R*)-$Cp(CO)_2FeC^*H(OCH_3)C_6H_5$ is used, racemization at the chiral Cα carbon can occur in the 16e intermediate presumably via α-elimination to a carbene–hydride intermediate. These observations illustrate that $Cp(CO)(PPh_3)Fe$– derivatives are not always configurationally stable[25] at 25 °C and that configurational integrity at Cα in metal alkyl complexes can be lost via α-elimination processes.

Experimental Section

All manipulations were performed under a nitrogen atmosphere by standard or modified Schlenk techniques unless otherwise noted. NMR spectra were recorded on either an IBM AC-200, a Bruker WM-250, or a Varian XL-400 with residual protonated solvent peaks as references ($CD\mathit{H}Cl_2$ δ 5.32, $C_6D_5\mathit{H}$ δ 7.15, $C_6D_5CD_2\mathit{H}$ δ 2.09). Infrared spectra were recorded on a Beckmann 4253 spectrophotometer with the polystyrene absorbance at 1601 cm^{-1} as reference. Optical rotations were measured at ambient temperature in 5 mL jacketed quartz cells on a Perkin-Elmer Model 241 polarimeter. Photolyses were performed with a sunlamp (GE H100PFL44-4 Reflector Flood Lamp). Solvents were purified and rendered oxygen-free by distillation under nitrogen atmosphere with either sodium/benzophenone (THF, hexanes, Et_2O, benzene, toluene), P_2O_5 (CH_2Cl_2), or Mg/magnesium methoxide (CH_3OH). NMR solvents were degassed by successive freeze/pump/thaw cycles and stored under nitrogen. PEt_3 was used as received from Strem and stored under nitrogen. All other reagents were used as received. (*S*)-(+)-*O*-Methylmandeloyl chloride,[26] $Cp(CO)_2Fe^-M^+$,[27] $Cp(CO)_2FeCOC_6H_5$,[28] $Cp(CO)_2FeCH(OCH_3)C_6H_5$,[29] $Cp(CO)(PPh_3)FeCOC_6H_5$,[30] and $Cp(CO)Fe[\eta^3\text{-}CH(OCH_3)C_6H_5]$[10] were prepared according to literature methods. Elemental analyses were performed by Galbraith Laboratories, Knoxville, TN, or University College Microanalytical Services, Dublin, Ireland.

$Cp(CO)_2FeCOCH(OCH_3)C_6H_5$ (5). A solution of 2.20 g (0.012 mmol) of *O*-methylmandeloyl chloride in 10 mL of THF was added dropwise to a rapidly stirred −78 °C solution of $Cp(CO)_2Fe^-M^+$ (2.59 g, 0.012 mmol) in 75 mL of THF. The mixture was warmed to 0 °C and transferred into a separatory funnel containing 100 mL of aqueous bicarbonate and 100 mL of CH_2Cl_2. After extraction, the bottom CH_2Cl_2 layer was collected. The aqueous layer was extracted two times with 50 mL of CH_2Cl_2. The CH_2Cl_2 extracts were combined, dried over anhydrous K_2CO_3, and filtered, and solvent was removed in vacuo, leaving a dark red-orange crude oil as product. Elution on neutral alu-

---

(24) Using the reaction conditions described by Davies[2] (i.e. 1 equiv of LAH or $NaBH_4$ in THF at −78 °C for reduction of $Cp(CO)(PPh_3)Fe{=}C(OCH_3)(Et)^+$), we observed overreduction of **15** and **16**, yielding $Cp(CO)(PPh_3)FeCH_2C_6H_5$ and $Cp(CO)(PEt_3)FeCH_2C_6H_5$ as the major products. We carried out our studies using our standard reduction method, which utilized $NaBH_4$ dissolved in $CH_3OH/CH_3O^-Na^+$. No overreduced products were observed using this method.

(25) Reger, D. L.; Culbertson, E. C. *Inorg. Chem.* **1977**, *16*, 3104.

(26) Mosher, H. S.; Dale, T. A. *J. Am. Chem. Soc.* **1973**, *95*, 512.

(27) Studabaker, W. B. Ph.D. Dissertation, University of North Carolina at Chapel Hill, Chapel Hill, NC, 1986.

(28) (a) King, R. B. *J. Am. Chem. Soc.* **1963**, *85*, 1918. (b) King, R. B. *J. Organomet. Chem.* **1964**, *2*, 15.

(29) (a) Brookhart, M.; Nelson, G. O. *J. Am. Chem. Soc.* **1977**, *99*, 6099. (b) Brookhart, M.; Studabaker, W. B.; Humphrey, M. B.; Husk, G. R. *Organometallics*, in press.

(30) Humphrey, M. B. Ph.D. Dissertation, University of North Carolina at Chapel Hill, Chapel Hill, NC, 1982.

mina with benzene gave a purple band ($[\mathrm{Cp(CO)_2Fe}]_2$). Further elution with $\mathrm{Et_2O}$ gave a bright yellow band of **5**. Solvent was removed, leaving a yellow-brown oil, which when dissolved in hexanes and cooled to −40 °C yielded 3.32 g (85% yield) of pure yellow crystalline product. ^{1}H NMR ($\mathrm{C_6D_6}$): δ 3.20 (s, 3 H, $-\mathrm{OC}H_3$), 4.04 (s, 5 H, η^5-$\mathrm{C_5}H_5$), 4.37 (s, 1 H, $-\mathrm{C}H$), 7.0–7.5 (m, 5 H, $-\mathrm{C_6H_5}$). ^{13}C NMR ($\mathrm{C_6D_6}$): δ 57.4 ($-\mathrm{O}C\mathrm{H_3}$), 86.9 (η^5-$C_5\mathrm{H_5}$), 99.5 ($-C\mathrm{H}$), 128.8, 128.5, 128.4, 128.1 ($C_6\mathrm{H_5}$), 215.8 ($-C\mathrm{OR}$), 257.2 ($-C\mathrm{O}$). IR ($\mathrm{CH_2Cl_2}$): ν_{CO} 2010, 1960; ν_{acyl} 1627 cm^{-1}. Anal. Calcd for $\mathrm{C_{16}H_{14}O_4Fe}$: C, 58.93; H, 4.33. Found: C, 59.07; H, 4.36. Optical rotation: (*S*)-**5** $[\alpha]_{\mathrm{D}} = -90°$.

$\mathrm{Cp(CO)(PPh_3)FeCH(OCH_3)C_6H_5}$ (4) from (*S*)-5. A 30-mL hexanes solution of (*S*)-**5** (317 mg, 0.97 mmol) and 262 mg (1.0 mmol) of $\mathrm{PPh_3}$ was added to a Pyrex photolysis tube, purged with nitrogen, and photolyzed with a sunlamp for 50 min. The reaction was monitored by IR spectroscopy. The absorption bands for (*S*)-**5** (2010, 1960, and 1627 cm^{-1}) disappeared as a single band for **4** (1901 cm^{-1}) grew in. Complex **4** is only slightly soluble in hexanes and precipitates out of solution. It is isolated by filtration as a pale orange powder (430 mg, 85% yield) and was identified as only a single diastereomer by NMR in agreement with spectral data previously reported[5] and had an optical rotation of $[\alpha]_{436} = 0°$.

$\mathrm{Cp(CO)(PEt_3)FeCH(OCH_3)C_6H_5}$ (7) from (*S*)-5. A 60-mL benzene solution of (*S*)-**5** (572 mg, 1.75 mmol) and $\mathrm{PEt_3}$ (700 μL, 4.8 mmol) was added to a Pyrex photolysis tube, purged with nitrogen, and photolyzed with a sunlamp. The reaction was monitored by IR spectroscopy. The absorption bands of (*S*)-**5** (2010, 1960, and 1627 cm^{-1}) disappeared as a single absorption band for **7** (1920 cm^{-1}) grew in. As the reaction proceeded, the initial yellow solution turned deep red. Solvent was removed in vacuo, giving a dark red oil, which was extracted with hexanes and filtered through Celite. Solvent removal gave a pure deep red oil as product (550 mg, 81%, 3:2 *SR*:*RS* to *SS*:*RR* diastereomer mixture). The (*SR*)-**7**:(*RS*)-**7** and (*SS*)-**7**:(*RR*)-**7** diastereomers were separated by −50 °C chromatography on Activity II–III basic alumina with 25:1 hexanes/$\mathrm{Et_2O}$. The (*SS*)-**7**:(*RR*)-**7** diastereomer eluted first. Dark red crystalline material was obtained from $\mathrm{CH_2Cl_2}$/2-methylbutane at −40 °C.

^{1}H NMR ($\mathrm{C_6D_6}$): *SR*:*RS* δ 4.91 (d, 1 H, $^3J_{\mathrm{PH}} = 8.8$ Hz, $-\mathrm{C}H$), 4.08 (s, 5 H, η^5-$\mathrm{C_5}H_5$), 3.13 (s, 3 H, $-\mathrm{OC}H_3$), 1.20 (dq, 6 H, P–$\mathrm{C}H_2$–), 0.70 (dt, 9 H, *p*-$\mathrm{CH_2C}H_3$), 7.0–7.5 (m, 5 H, $-\mathrm{C_6}H_5$); *SS*:*RR* δ 5.31 (d, 1 H, $^3J_{\mathrm{PH}} = 6.7$ Hz, $-\mathrm{C}H$), 3.85 (s, 5 H, η^5-$\mathrm{C_5}H_5$), 2.49 (s, 3 H, $-\mathrm{OC}H_3$), 1.45 (dq, 6 H, P–$\mathrm{C}H_2$–), 0.90 (dt, 9 H, P–$\mathrm{CH_2C}H_3$), 7.0–7.5 (m, 5 H, $-\mathrm{C_6}H_5$). ^{13}C NMR ($\mathrm{CD_2Cl_2}$): *SR*:*RS* δ 83.42 (η^5-$C_5\mathrm{H_5}$), 78.70 ($-C\mathrm{H}$), 58.52 ($-\mathrm{O}C\mathrm{H_3}$), 20.09 (d, $^2J_{\mathrm{PC}} = 25.1$ Hz, P–$C\mathrm{H_2}$–), 7.65 (d, $^3J_{\mathrm{PC}} = 2.4$ Hz, P–$\mathrm{CH_2}C\mathrm{H_3}$); *SR*:*RS* δ 83.16 (η^5-$C_5\mathrm{H_5}$), 81.19 ($-C\mathrm{H}$), 58.28 ($-\mathrm{O}C\mathrm{H_3}$), 17.72 (d, $^2J_{\mathrm{PC}} = 24.1$ Hz, P–$C\mathrm{H_2}$–), 7.29 (P–$\mathrm{CH_2}C\mathrm{H_3}$). IR (hexanes): ν_{CO} *SR*:*RS* 1925 cm^{-1}; *SS*:*RR* 1915 cm^{-1}. Optical rotation: (*RR*)-**7** $[\alpha]^{23}{}_{436} = +740°$; (*SR*)-**7** $[\alpha]^{23}{}_{436} = -720°$. Anal. Calcd for $\mathrm{C_{20}H_{29}O_2PFe}$: C, 61.88; H, 7.48. Found: C, 61.85; H, 7.58.

Rate of $\mathrm{PPh_3}$ Dissociation from (*SS*)-4:(*RR*)-4. In a 5-mm NMR tube, $\mathrm{Cp(CO)_2FeCH(OCH_3)C_6H_5}$ (**3**) (7 mg, 2.3×10^{-2} mmol) in 400 μL of toluene-d_8 was photolyzed for 15 min at −75 °C, forming a deep red solution of **9**. A solution of 6 mg (2.3×10^{-2} mmol) of $\mathrm{PPh_3}$ in 110 μL of toluene-d_8 was added at −75 °C and nitrogen bubbled through the solution to facilitate mixing. The sample was warmed until the dark red color of **9** discharged to clear orange **4** (<1 min) and then recooled to −75 °C; 20 μL (0.137 mmol) of $\mathrm{PEt_3}$ was added and nitrogen bubbled through to mix. The sample was frozen in liquid nitrogen, sealed under vacuum, and then warmed to 293 K and immediately placed in the NMR probe. The rate of $\mathrm{PPh_3}$ dissociation from (*SS*)-**4**:(*RR*)-**4** was measured over time by recording successive ^{1}H NMR spectra at 293 K. The first-order disappearance of the $-\mathrm{OC}H_3$ singlet at δ 2.37 for (*SS*)-**4**:(*RR*)-**4** versus internal standard $\mathrm{C_6D_5CD_2}H$ at δ 2.09 was determined by integration. A plot of −ln [(*SS*)-**4**:(*RR*)] versus time (seconds) yielded a rate of $\mathrm{PPh_3}$ dissociation from (*SS*)-**4**:(*RR*)-**4** of 1.3×10^{-4} s^{-1} (since the molar excess of $\mathrm{PEt_3}$ is approximately 7-fold, it is safe to assume pseudo-first-order kinetics where $\mathrm{PEt_3}$ traps **6** as soon as $\mathrm{PPh_3}$ dissociates with no $\mathrm{PPh_3}$ retrapping to reform **4**), giving $t_{1/2} = 87.5$ min and $\Delta G^{\ddagger}$ ((*SS*)-**4**:(*RR*)-**4**) = 22.3 kcal/mol ($T = 293$ K).

Rate of $\mathrm{PPh_3}$ Dissociation from (*SR*)-4:(*RS*)-4. To a 500-μL toluene-d_8 solution of 75:1, (*SR*)-**4**:(*RS*)-**4** to (*SS*)-**4**:(*RR*)-**4** (8 mg, 1.5×10^{-2} mmol), in a 5-mm TMR tube was added $\mathrm{PEt_3}$ (30 μL, 0.206 mmol). The sample was shaken, frozen in liquid nitrogen, and sealed under vacuum. The rate of $\mathrm{PPh_3}$ dissociation from (*SR*)-**4**:(*RS*)-**4** was measured by recording successive ^{1}H NMR spectra at 293 K. The first-order disappearance of the $-\mathrm{C}H$ peak at δ 5.09 for (*SR*)-**4**:(*RS*)-**4** versus internal standard $\mathrm{C_6D_5CD_2}H$ at δ 2.09 was measured by integration. A plot of −ln [(*SR*)-**4**:(*RS*)-**4**] versus time (seconds) yielded a rate of $\mathrm{PPh_3}$ dissociation from (*SR*)-**4**:(*RS*)-**4** of 3.1×10^{-6} s^{-1} (since the molar excess of $\mathrm{PEt_3}$ is approximately 7-fold, it is safe to assume pseudo-first-order reaction kinetics where $\mathrm{PEt_3}$ traps **6** as soon as $\mathrm{PPh_3}$ dissociates with no $\mathrm{PPh_3}$ retrapping to reform **2**), giving $t_{1/2} = 61$ h and $\Delta G^{\ddagger} = 24.5$ kcal/mol at $T = 293$ K.

Methoxide Addition to $\mathrm{Cp(CO)(PR_3)Fe{=}CHC_6H_5^+}$. $\mathrm{PR_3 = PPh_3}$. General Procedure. In a 5-mm NMR tube, $\mathrm{CF_3COOH}$ (3 μL, 3×10^{-2} mmol, 2 equiv) was added to a −78 °C solution of **4** (8 mg, 1.5×10^{-2} mmol) in 450 μL of $\mathrm{CD_2Cl_2}$ to form a deep red solution of **11**. The solution of **11** was added dropwise to 250 μL of a $\mathrm{CD_3OD/CD_3O^-Na^+}$ solution (of specified concentration) in a 5-mm NMR tube cooled to 0 °C, which was being purged with nitrogen to facilitate complete and rapid mixing. Upon addition, the deep red discharged to form a clear orange solution, which was immediately cooled to −78 °C, sealed under vacuum, and maintained at −78 °C until a ^{1}H NMR spectrum was recorded at −42 °C. ^{1}H NMR showed the product to be pure **4** with no significant side products. Diastereomer ratios were determined by integration of the $-\mathrm{C}H$ peaks in the spectrum at δ 4.71 ($^3J_{\mathrm{PH}} = 9.8$ Hz) for (*SR*)-**4**:(*RS*)-**4** and δ 5.01 ($^3J_{\mathrm{PH}} = 6.8$ Hz) for (*SS*)-**4**:(*RR*)-**4** ($\mathrm{CD_2Cl_2/CD_3OD}$) and are summarized in Table II.

$\mathrm{PR_3 = PEt_3}$. General Procedure. $\mathrm{CF_3COOH}$ (12 μL, 1.6×10^{-1} mmol, 2 equiv) was added to a −45 °C solution of **7** (30 mg, 7.7×10^{-2} mmol) in 3 mL of $\mathrm{CH_2Cl_2}$ to generate a dark red solution of **12**. The solution of **12** was added dropwise to a rapidly stirring $\mathrm{CH_3OH/CH_3O^-Na^+}$ solution (of specified concentration) at 0 °C with the deep red color discharging to give a clear yellow solution. A total of 10 mL of $\mathrm{CH_2Cl_2}$ and 10 mL of aqueous bicarbonate was added, the solution mixed, and the bottom $\mathrm{CH_2Cl_2}$ layer filtered through a plug of Celite/anhydrous $\mathrm{K_2CO_3}$. Solvent removal in vacuo yielded 28 mg (94%) of red-orange oil product. ^{1}H NMR ($\mathrm{C_6D_6}$) showed the product to be pure **7** with no evidence of other products. Diastereomer ratios were determined by integration of the $-\mathrm{C}H$ peak at δ 4.91 ($^3J_{\mathrm{PH}} = 8.8$ Hz) for (*SR*)-**7**:(*RS*)-**7** and δ 5.30 ($^3J_{\mathrm{PH}} = 6.8$ Hz) for (*SS*)-**7**:(*RR*)-**7** and are summarized in Table II.

$\mathrm{Cp(CO)(PEt_3)FeCR(OCH_3)C_6H_5}$ [7, R = H; [α-*D*]-7, R = D]. General Procedure. A Pyrex photolysis tube containing a 50-mL benzene solution of 500 mg (1.68 mmol) of $\mathrm{Cp(CO)_2FeCR(OCH_3)C_6H_5}$ (**3** or [α-*D*]-**3**) and 735 μL (5.04 mmol) of $\mathrm{PEt_3}$ was photolyzed with a sunlamp. The reaction was complete when the IR bands for **3** (or [α-*D*]-**3**) at 2010 and 1960 cm^{-1} disappeared and a new band at 1905 cm^{-1} for $\mathrm{Cp(CO)(PEt_3)FeCR(OCH_3)C_6H_5}$ grew in. Solvent was removed in vacuo, the product red oil was redissolved in $\mathrm{Et_2O}$ and filtered through a plug of Celite, and solvent was removed to leave 555 mg (85% yield) of a 3:2 *SR*:*RS* to *SS*:*RR* diastereomer mixture of pure product as a red-orange oil. Spectral data for **7** and [α-*D*]-**7** prepared by this method matched those reported earlier. [α-*D*]-**7** lacked the ^{1}H NMR resonances for the α-hydrogen ($-\mathrm{C}H$), indicating complete deuteriation at that site (≥95%). ^{2}H NMR for [α-*D*]-**7** ($\mathrm{C_6H_6}$): δ 4.90 (s, 1 H, $-\mathrm{C}D$), for [α-*D*]-(*SR*)-**7**:[α-*D*]-(*RS*)-**7**; δ 5.30 (s, 1 H, $-\mathrm{C}D$), for [α-*D*]-(*SS*)-**7**:[α-*D*]-(*RR*)-**7**.

$\mathrm{LiDBEt_3}$ Addition to $\mathrm{Cp(CO)(PEt_3)Fe{=}CHC_6H_5^+CF_3COO^-}$ (12). $\mathrm{CF_3COOH}$ (20 μL, 2.60 mmol) was added to a −45 °C solution of **7** (100 mg, 0.258 mmol) in 5 mL of $\mathrm{CH_2Cl_2}$ to generate a dark red solution of **12**. Upon addition to 800 μL of a 1.0 M $\mathrm{LiDBEt_3}$ in THF solution at −45 °C, the red color immediately discharged to give a yellow-orange solution. A total of 10 mL of $\mathrm{CH_2Cl_2}$ was added and the solution filtered through Celite. Solvent removal in vacuo yielded 85 mg (92% yield) of bright yellow powder. The diastereomer ratio of the product $\mathrm{Cp(CO)(PEt_3)FeCH(D)C_6H_5}$ (**15**) was determined by ^{1}H and ^{2}H NMR integration of the peaks for the benzylic protons ($-\mathrm{C}HD$). The NMR data are given in Table III.[31]

$\mathrm{LiHBEt_3}$ Addition to $\mathrm{Cp(CO)(PEt_3)Fe{=}CDC_6H_5^+CF_3COO^-}$ ([α-*D*]-12). The experiment was performed as described above using 80 mg of (0.206 mmol) [α-*D*]-**7** to generate deuteriobenzylidene [α-*D*]-**12** and a 1.0 M solution of $\mathrm{LiHBEt_3}$ in THF. The yield of $\mathrm{Cp(CO)(PEt_3)FeCD(H)C_6H_5}$ (**15**) was 69 mg (94% yield). ^{1}H and ^{2}H NMR data for the products are given in Table III.

$\mathrm{Cp(CO)(PEt_3)FeCOC_6H_5}$ (21). A 50-mL benzene solution of $\mathrm{Cp(CO)_2FeCOC_6H_5}$ (513 mg, 1.8 mmol) and $\mathrm{PEt_3}$ (300 μL, 2.1 mmol) in a Pyrex apparatus was photolyzed with a sunlamp for 1 h with a nitrogen purge through the solution. The solution turned from clear yellow to clear orange. The progress of the reaction was monitored by IR spectroscopy. The absorption bands for $\mathrm{FpCOC_6H_5}$ (2020, 1960, and 1620 cm^{-1}) disappeared while absorption bands for $\mathrm{Cp(CO)(PEt_3)FeC_6H_5}$ (1910 and 1565 cm^{-1}) and **21** (1915 and 1565 cm^{-1}) appeared. Solvent was removed in vacuo and the crude red oily product chromatographed on alumina with 15:1 hexanes/ethyl acetate. The first band to elute was

---

(31) $\mathrm{Cp(CO)(PEt_3)Fe\text{-}CH_2C_6H_5}$. ^{1}H NMR ($\mathrm{C_6D_4CD_3}$): δ 0.80 (dt, 9 H, $J = 14.2, 7.4$ Hz, P–$\mathrm{CH_2C}H_3$), 1.19 (m, 6 H, P–$\mathrm{C}H_2$), 1.70 (dd, 1 H, $J = 8, 8$ Hz, C*H*H′), 2.26 (dd, 1 H, $J = 8, 5$ Hz, CH*H*′), 3.65 (s, 5 H, η^5-$\mathrm{C_5}H_5$), 7.06–7.37 (m, 5 H, $\mathrm{C_6}H_5$). Full spectral data and characterization appear in the following paper.

yellow $Cp(CO)(PEt_3)FeC_6H_5$. A second yellow band, eluted with 5:1 hexanes/ethyl acetate, was **21**. Solvent was removed in vacuo, and the product oils were redissolved in hexane and cooled to –40 °C. Orange crystalline material was obtained for both products. Yield: 280 mg of **21** (41%); 200 mg of $Cp(CO)(PEt_3)FeC_6H_5$ (32%).

21. ^{1}H NMR (C_6D_6): δ 0.73 (dt, 9 H, J = 7.5, 15 Hz, P–CH_2CH_3), 1.31 (dq, 3 H, J = 7.5, 22.5 Hz, P–CHH'–), 1.51 (dq, 3 H, J = 7.5, 22.5 Hz, P–CHH'–), 4.30 (s, 5 H, Cp), 7.18 (t, 1 H, J = 7.3 Hz, H(para)), 7.31 (dd, 2 H, J = 7.6, 7.6 Hz, H(meta)), 7.99 (d, 2 H, J = 7.6 Hz, H(ortho)). IR (CH_2Cl_2): ν_{CO} 1912, 1590, 1575, 1550 cm^{-1}. Anal. Calcd $C_{19}H_{25}O_2PFe$: C, 61.31; H, 6.77. Found: C, 60.93; H, 6.91.

Synthesis of $Cp(CO)(PR_3)Fe{=}C(OCH_3)C_6H_5^+OTf^-$ (17, R = Ph; 18, R = Et). General Procedure.[32] $(\eta^5\text{-}C_5H_5)(CO)(PR_3)FeCOC_6H_5$ was dissolved in CH_2Cl_2 and 2 equiv of MeOTf added. After it was stirred at room temperature overnight, the solution turned from clear orange to deep red. The reaction was deemed complete by IR spectroscopy when the acyl (1560 cm^{-1}) and carbonyl (1910 cm^{-1}) absorption bands of the starting benzoyl disappeared and a single absorption band at 1985 cm^{-1} for the heterocarbene grew in. The reaction mixture was filtered through Celite, solvent was removed in vacuo, and the product dark red oil was washed several times with Et_2O.

17. ^{1}H NMR (CD_2Cl_2): δ 3.39 (s, 3 H, –OCH_3), 4.96 (d, 5 H, $^3J_{PH}$ = 1.2 Hz, η^5-C_5H_5), 6.93–8.09 (m, 20 H, –C_6H_5's). ^{13}C NMR (CD_2Cl_2): δ 60.8 (–OCH_3), 87.9 (η^5-C_5H_5), 127.2–134.6 (C_6H_5's), 152.0 (C(ipso) of carbene phenyl), 217.0 (d, $^2J_{PC}$ = 28.7 Hz, –CO), 333.6 (d, $^2J_{PC}$ = 24.7 Hz, =C). IR (CH_2Cl_2): ν_{CO} 1984 cm^{-1}.

18. ^{1}H NMR (CD_2Cl_2): δ 1.03 (dt, 9 H, J = 7.7, 16.2 Hz, P–CH_2CH_3), 1.85 (m, 6 H, P–CH_2), 3.48 (s, 3 H, –OCH_3), 5.09 (d, 5 H, $^3J_{PH}$ = 1.2 Hz, η^5-C_5H_5), 7.44–7.60 (m, 5 H, –C_6H_5). ^{13}C NMR (CD_2Cl_2): δ 8.11, P–CH_2CH_3), 21.7 (d, $^1J_{PC}$ = 28.6 Hz, P–CH_2–), 61.3 (–OCH_3), 86.8 (η^5-C_5H_5), 133.9, 128.9, 127.2 (C(ortho), C(meta), C(para)), 152.7 (C(ipso)), 216.5 (d, $^2J_{PC}$ = 28.8 Hz, –CO), 331.6 (d, $^2J_{PC}$ = 21.2 Hz, =C). IR (CH_2Cl_2): ν_{CO} 1988 cm^{-1}.

Hydride Addition to $Cp(CO)(PR_3)Fe{=}C(OCH_3)C_6H_5^+$. 17: $PR_3 = PPh_3$. General Procedure. A 450-μL CD_2Cl_2 solution of **17** (10 mg, 1.9 × 10^{-2} mmol) was prepared in a 5-mm NMR tube at room temperature and added dropwise to 250 μL of a $CD_3OD/CD_3O^-Na^+/NaBH_4$ solution[23] (of the specified $NaBH_4$ concentration) cooled to either 0 or –78 °C, which was purged with nitrogen to facilitate complete and rapid mixing. (All solutions had a 5:1 molar ratio of $NaBH_4$ to $NaOCD_3$.) Upon addition, the deep red color of the heterocarbene discharged immediately to clear orange. When addition was complete, the sample was immediately cooled to –78 °C, sealed under vacuum, and maintained at –78 °C until a ^{1}H NMR spectrum at –42 °C could be recorded. ^{1}H NMR showed the product to be pure **4** with no side products. Diastereomer ratios were determined by ^{1}H NMR integration of the –CH peaks at δ 4.71 for (SR)-**4**:(RS)-**4** and δ 5.01 for (SS)-**4**:(RR)-**4** and are summarized in Table IV.

18: $PR_3 = PEt_3$. General Procedure. A 3-mL CH_2Cl_2 solution of **18** (30 mg, 5.6 × 10^{-2} mmol) was added dropwise to 1 mL of a rapidly stirring $CH_3OH/CH_3O^-Na^+/NaBH_4$ solution (of specified concentration) at 0 °C. (All solutions were 5:1 $NaBH_4/NaOCH_3$.) Immediate discharge of the deep red carbene to clear yellow occurred. A total of 10 mL of CH_2Cl_2 and 10 mL of aqueous bicarbonate was added, the solution stirred rapidly, and the bottom CH_2Cl_2 layer filtered through a plug of Celite/anhydrous K_2CO_3. Solvent was removed in vacuo, yielding 20.2 mg (93%) of red-orange oil. ^{1}H NMR (C_6D_6) showed the product to be pure **7**. Diastereomer ratios were determined by integration of the –CH peaks at δ 4.91 for (SR)-**7**:(RS)-**7** and δ 5.30 for (SS)-**7**:(RR)-**7** and are summarized in Table IV.

Acknowledgment is made to the donors of the Petroleum Research Fund, administered by the American Chemical Society, and to the National Institutes of Health (Grant GM-23938) for the support of this research.

Registry No. 3, 64494-50-4; [α-D]-**3**, 117094-47-0; **4** (isomer 1), 113350-82-6; **4** (isomer 2), 104832-41-9; (S)-**5**, 117094-46-9; (S)-**6**, 55137-68-3; **7**, 117178-89-9; **7** (isomer 1), 113215-01-3; **7** (isomer 2), 113109-99-2; [α-D]-**7** (isomer 1), 117094-48-1; [α-D]-**7** (isomer 2), 117178-90-2; **9**, 117180-25-3; **11A**, 113214-96-3; **11S**, 113214-94-1; **12A**, 117178-88-8; **12S**, 117178-92-4; [α-D]-**12A**, 117094-51-6; [α-D]-**12S**, 117178-94-6; **15** (isomer 1), 117094-49-2; **15** (isomer 2), 117178-91-3; **17**, 117094-55-0; **18**, 117094-57-2; **21**, 117094-53-8; $Cp(CO)_2Fe^-K^+$, 60039-75-0; $Cp(CO)_2FeCOC_6H_5$, 12154-94-8; $Cp(CO)(PPh_3)FeCOC_6H_5$, 12118-59-1; $Cp(CO)(PEt_3)FeC_6H_5$, 117094-52-7.

---

[32] Cutler, A. R.; Bodnar, T. W. *Synth. React. Inorg. Met.-Org. Chem.* **1985**, *15*(1), 31.

Synthesis, Spectroscopic Characterization, Dynamics, and Phosphine Trapping of $Cp(CO)Fe[\eta^3\text{-}CH(R)C_6H_5]$ Complexes ($R = H, OCH_3$)

M. Brookhart,* Robert C. Buck, and Earl Danielson, III

Contribution from the Department of Chemistry, The University of North Carolina at Chapel Hill, Chapel Hill, North Carolina 27599-3290. Received March 7, 1988

Abstract: Low-temperature photolysis of $Cp(CO)_2FeCH(R)C_6H_5$ (**1A**, R = H; **1B**, R = OCH_3) yields η^3-benzyl complexes $Cp(CO)Fe(\eta^3\text{-}CH(R)C_6H_5)$ (**3A**, R = H; **3B**, R = OCH_3), respectively, which have been characterized by ^{1}H and ^{13}C NMR spectroscopy. The dynamic behavior of **3A** and **3B** has been studied by variable-temperature ^{1}H NMR spectroscopy. The free energies of activation for the formation of the η^1 species $Cp(CO)Fe(\eta^1\text{-}CH(R)C_6H_5)$ (**2A**, R = H; **2B**, R = OCH_3) from **3A** and **3B** were determined as 12.0 and 15.4 kcal/mol, respectively. When an excited-state absorption spectrophotometric experiment was used, the η^1 species **2A** could be generated from **1A** and its rate of collapse to **3A** measured as 1 × 10^8 s^{-1} at 293 K. The equilibrium ratio of **3A**:**2A** was estimated as ca. 10^4 at 293 K. Kinetics of trapping of **3A** and **3B** by $P(C_6H_5)_3$ and $P(C_2H_5)_3$ were carried out under pseudo-first-order conditions at low temperatures (202 and 231 K). These data coupled with information from dynamic NMR and flash photolysis studies and, for $P(C_6H_5)_3$, rates of dissociation allow a complete thermodynamic and kinetic description of several of these systems (see free energy diagrams in Figures 4 and 5).

In the preceding paper an investigation of three synthetic routes to chiral-at-iron complexes $Cp(CO)(PR_3)FeCH(OCH_3)C_6H_5$ (R = Ph, Et) was reported.[1] These complexes represent precursors to cationic chiral-at-iron benzylidene complexes, which have been shown to transfer the benzylidene fragment to olefins enantioselectively.[2] One of the routes to these complexes involved the photochemical ligand substitution of $Cp(CO)_2FeCH(OCH_3)C_6H_5$ (**1B**) with PPh_3 and PEt_3. The iron η^3-benzyl complex $Cp(CO)Fe[\eta^3\text{-}CH(OCH_3)C_6H_5]$ (**3B**) was detected as an interme-

---

[1] Brookhart, M.; Buck, R. C. *J. Am. Chem. Soc.*, preceding paper in this issue.

[2] (a) Buck, R. C.; Brookhart, M. *Abstracts of Papers*, 191st National Meeting of the American Chemical Society, New York, April 13–18, 1986; American Chemical Society: Washington, DC, 1986; INORG 422. (b) The corresponding chiral-at-iron ethylidene complexes have also been shown to transfer ethylidene to olefins to form cyclopropanes of high enantiomeric purity: Brookhart, M.; Timmers, S.; Tucker, J. R.; Williams, G. D.; Husk, G. R.; Brunner, H.; Hammer, B. *J. Am. Chem. Soc.* **1983**, *105*, 6721.

0002-7863/89/1511-0567$01.50/0 © 1989 American Chemical Society